

000 001 002 003 004 005 DIVERSITY MATTERS: REVISITING TEST-TIME COM- 006 PUTE IN VISION-LANGUAGE MODELS 007 008 009

010 **Anonymous authors**
011
012
013
014
015
016
017
018
019
020
021
022
023
024
025
026
027
028
029
030
031
032
033
034
035
036
037
038
039
040
041
042
043
044
045
046
047
048
049
050
051
052
053

Paper under double-blind review

ABSTRACT

Test-time compute (TTC) strategies have emerged as a lightweight approach to boost reasoning in large language models, but their applicability to vision-language models (VLMs) remains unclear. We present a systematic study of TTC for visual reasoning across seven open-source VLMs and six benchmarks, revisiting two paradigms: (i) feature-based scoring of chain-of-thought (CoT) traces and (ii) confidence-based aggregation via majority voting (MV). In the single-model setting, feature cues (e.g., length, pivot words) fail to improve accuracy, while MV yields only modest, CoT-dependent gains. To explain this limitation, we theoretically show that the voting method’s effectiveness depends on *prediction diversity*: when outputs are highly correlated, the benefit of voting vanishes. In contrast, *multi-model ensembles* introduce stronger diversity through architectural differences, training data, and scale, making them both more realistic and more promising for TTC. However, MV treats all models equally, leaving it vulnerable to correlated errors from weaker models. To address this, we propose *Entropy-based TTC*, which selects the most confident prediction based on predictive entropy. Our method reduces to MV in the single-model case but, in ensembles, leverages confidence disparities to prioritize stronger models. We prove that our method theoretically outperforms MV under mild dependence assumptions, and empirically show that it consistently surpasses both MV and the best individual model across diverse visual reasoning benchmarks. This demonstrates that smaller models can enhance, rather than hinder, larger ones when combined appropriately, unlocking ensemble gains not achievable with existing TTC strategies.

1 INTRODUCTION

Vision-Language Models (VLMs) have recently achieved remarkable performance across a range of visual reasoning benchmarks (Llama Team, 2024; Agrawal et al., 2024; Gemma Team, 2025; Bai et al., 2025; OpenAI, 2023; Gemini Team, 2025). At the same time, the large language modeling (LLM) community has developed a family of *test-time compute* (TTC) strategies, particularly those based on *chain-of-thought* (CoT) prompting, to improve reasoning without modifying model parameters (Snell et al., 2024). These strategies generate multiple outputs per input and then aggregate or rank them to produce more reliable predictions.

In the LLM literature, TTC methods fall broadly into two categories. *Feature-based* methods attempt to estimate the quality of each CoT reasoning trace by analyzing textual signals, such as the presence of specific pivot words (Chang et al., 2025; Lippmann & Yang, 2025), confident linguistic tone (Mao et al., 2025), or the length of the reasoning chain (Fu et al., 2023; Jin et al., 2024). In contrast, *confidence-based* methods treat the model as a stochastic oracle and improve reasoning reliability by aggregating multiple outputs, typically selecting the most frequent answer across samples via voting (Wang et al., 2023; Chen et al., 2024b; Snell et al., 2024).

Applying TTC to VLMs, however, is far from straightforward. Unlike LLMs, VLMs must first perceive and interpret dense visual signals before reasoning over them. This introduces new challenges: (i) visual perception is inherently error-prone and varies across models (Bhattacharyya et al., 2023; Wang et al., 2025); (ii) vision-language alignment remains imperfect, creating subtle inconsistencies (Li et al., 2025; Yan et al., 2025); and (iii) textual cues that correlate with the correctness in LLM

054 may not reflect the true visual understanding (Al-Tahan et al., 2024; Jiang et al., 2025). Therefore, it
 055 is unclear whether and when TTC strategies can reliably enhance visual reasoning.
 056

057 To investigate this, we begin with the *single-model (multi-round)* setting, where one VLM is queried
 058 multiple times with randomness (§ 3). Our findings reveal that: (1) feature-based methods fail to
 059 improve accuracy, showing that linguistic style is a poor proxy for visual reasoning quality; and
 060 (2) confidence-based methods such as majority voting (MV) provide only modest, but consistent,
 061 gains, and only when CoT prompting is used. Without CoT, even aggregation brings no benefit.
 062

063 Why are these gains so limited? We analyze the *diversity* (formally, the *statistical dependency*) be-
 064 tween predictions and show that MV’s effectiveness decreases as predictions become more correlated
 065 (§ 4.1). When model outputs are nearly identical, voting cannot amplify the signal of correctness.
 066 Empirically, we confirm this across 7 VLMs and 6 datasets: outputs exhibit weak but nonzero
 067 dependency, which explains why MV offers only small improvements in practice (§ 4.2).
 068

069 These insights point to a deeper limitation: in the single-model setting, diversity arises only from
 070 sampling randomness, so the expected skill of the model remains unchanged. By contrast, *multi-*
 071 *model ensembles* naturally introduce stronger diversity: differences in architecture, training data, and
 072 even scale create complementary strengths. This makes ensembles both more realistic in practice and
 073 more promising for TTC. Existing methods, such as MV, cannot exploit this potential: by treating all
 074 models equally, MV risks letting weaker but correlated models dominate the outcome. What is needed
 075 is a strategy that adapts to model quality and selectively prioritizes the most reliable predictions.
 076

077 To address this, we introduce a new TTC strategy for visual reasoning: *Entropy-based Test-Time*
 078 *Consistency* (ETTC) (§ 5.1). Instead of counting votes, ETTTC selects the prediction with the lowest
 079 entropy (on the answer distribution from multiple responses), that is, the most confident output
 080 distribution. In the single-model setting, ETTTC reduces to MV, ensuring backward compatibility. But
 081 in multi-model ensembles, ETTTC diverges from MV: it leverages confidence gaps across models,
 082 allowing smaller models to assist stronger ones rather than overwhelm them. We theoretically prove
 083 that ETTTC outperforms MV under mild dependence assumptions (§ 5.2), and empirically show that it
 084 not only improves over MV but can even surpass the best individual model in the ensemble (§ 5.3).
 085 This result is particularly striking: *smaller models can be used to enhance larger ones when combined*
 086 *wisely*, yielding gains not achievable with MV alone.
 087

088 In summary, our contributions are:
 089

- 090 • A systematic theoretical and empirical study of TTC in VLMs, showing that feature cues fail and
 091 that MV yields only modest CoT-dependent gains (§ 3).
 092
- 093 • A theoretical analysis linking MV’s effectiveness to prediction dependency, supported by empirical
 094 evidence across diverse models and datasets (§ 4).
 095
- 096 • A new entropy-based method, ETTTC, that generalizes MV and achieves consistent improvements
 097 in multi-model ensembles, often surpassing even the best single model (§ 5).
 098

099 2 PREPARATION

100 We begin by outlining the models, datasets, prompting formats, TTC baselines, and general evaluation
 101 settings used in our experiments.
 102

103 **Models.** We evaluate seven open-source VLMs under two complementary multi-model ensemble
 104 configurations. In the *similar-size (cross-family)* setup, we include four VLMs with comparable
 105 parameter sizes but diverse architectures: Qwen2.5-VL-7B-Instruct (Bai et al., 2025, Qwen-7B),
 106 LLaMA-3.2-11B-Vision (Llama Team, 2024, LLaMA), Gemma-3-12B-it (Gemma Team, 2025,
 107 Gemma), and Pixtral-12B-2409 (Agrawal et al., 2024, Pixtral). In the *same-family (varied-size)* setup,
 108 we use four models from the Qwen2.5-VL-Instruct family (Bai et al., 2025), ranging from 3B to 72B
 109 parameters (3B, 7B, 32B, 72B), allowing us to study scaling effects within a single model family.
 110

111 **Datasets.** We experiment on six multiple-choice visual QA benchmarks covering three domains.
 112 For *math reasoning*, we use the testmini split of MathVista (Lu et al., 2024) and the test set of
 113 MathVision (Wang et al., 2024). For *diagram understanding*, we include the test sets of TQA (Kim
 114 et al., 2019) and ScienceQA (Lu et al., 2022). For *general visual reasoning*, we use the validation
 115

108 splits of MMStar (Chen et al., 2024a) and MMMU (Yue et al., 2024). All datasets contain multiple-
 109 choice QA instances with K answer options per question ($2 \leq K \leq 9$). Further statistics, including
 110 domain, split size, and option counts, are summarized in Tab. 3 in App. C.1.
 111

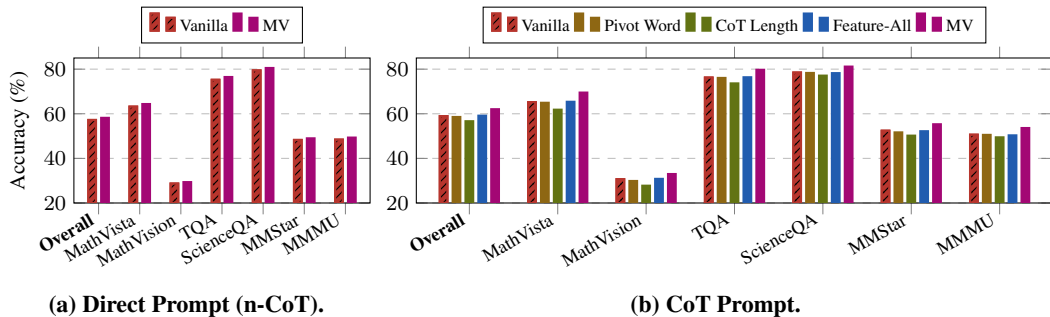
112 **Decoding.** We use decoding (Sutskever et al., 2014) via HuggingFace’s default generation set-
 113 tings.¹ We adopt two prompting formats: (1) *Non-CoT* (*n-CoT*) prompting discourages intermediate
 114 reasoning and elicits direct answers; (2) *Chain-of-thought* (*CoT*) prompting explicitly encourages
 115 step-by-step reasoning, followed by a final answer. We use zero-shot, one-stage prompting for both
 116 settings to ensure consistency across models. Full prompt templates are provided in Figs. 4 and 5 in
 117 App. C.2. Final answers are parsed via regex to extract discrete predictions.
 118

119 **TTC baselines.** To revisit TTC strategies for visual reasoning, we evaluate four representative
 120 baselines spanning feature-based and confidence-based approaches. Three are *feature-based* scoring
 121 methods applied to CoT responses: (1) *CoT Pivot Word* ranks each response by counting predefined
 122 reasoning-related expressions (e.g., “alternatively”) (Chang et al., 2025; Lippmann & Yang, 2025);
 123 see full phrase list in Tab. 4 of App. C.3. (2) *CoT Length* prefers longer responses, following prior
 124 work suggesting a correlation between length and reasoning quality (Fu et al., 2023). (3) *Feature-All*
 125 combines four interpretable features—pivot word count, vague word count, total token count, and
 126 lexical diversity—to compute a composite score (see Tab. 6). As a *confidence-based* method, (4)
 127 *Majority Voting* (*MV*) (Wang et al., 2023; Snell et al., 2024) aggregates $N = 16$ samples and selects
 128 the most frequent final answer (breaking ties randomly).
 129

130 **Evaluation settings.** We assess all TTC methods under two settings: (1) In the *single-model (multi-*
 131 *round)* setting, a single VLM is queried N times per question with stochasticity in decoding (e.g.,
 132 *CoT* sampling). TTC is used to aggregate these intra-model outputs. (2) In the *multi-model ensemble*
 133 setting, M distinct VLMs are queried per question (each with multiple samples), introducing both
 134 intra- and inter-model variation. This setting allows us to study cross-model complementarity and
 135 test whether aggregating weaker models can improve over any individual model.
 136

3 WHETHER TTC WORKS IN VISUAL REASONING

137 We begin by revisiting whether TTC strategies, widely used in LLMs, improve visual reasoning
 138 in VLMs. We evaluate four representative methods across six multiple-choice visual benchmarks
 139 and compare their performance under two prompting conditions: direct answering (*n-CoT*) and
 140 chain-of-thought reasoning (*CoT*). Results are averaged across seven VLMs unless otherwise noted.
 141



150 **(a) Direct Prompt (*n-CoT*).** **(b) CoT Prompt.**
 151
 152 Figure 1: Comparison of test-time compute (TTC) strategies under two prompting styles. In **n-CoT** (left),
 153 models are instructed to output only the final answer without reasoning; feature-based methods are inapplicable,
 154 and majority voting (MV) shows no improvement. In **CoT** (right), models are prompted to reason step by step.
 155 While feature-based methods yield no gains, MV offers modest but consistent improvement across datasets.

156 **Direct Prompt (*n-CoT*): TTC fails without CoT.** The *n-CoT* setting tests whether test-time
 157 variation alone, without prompting explicit reasoning, can boost accuracy. Since no reasoning chains
 158 are produced, only confidence-based methods like majority voting (MV) are applicable.
 159

160 As shown in Fig. 1 (left), MV provides negligible or no improvement over the greedy baseline (often
 161 <1%). Although we sample 16 outputs per question with stochastic decoding, the model’s predictions

¹https://huggingface.co/docs/transformers/en/generation_strategies

162 are mostly identical. This suggests that in the absence of CoT prompting, VLMs tend to output the
 163 same surface-level answer, showing little diversity in reasoning or interpretation. As a result, TTC
 164 offers no benefit under direct answering. This aligns with findings in LLMs (Wang et al., 2023; Snell
 165 et al., 2024), but is further exacerbated in VLMs due to the perception bottleneck, visual content must
 166 first be interpreted before any meaningful variation can emerge.

167
 168 **Chain-of-Thought Prompt (CoT): confidence helps, features don't.** In contrast, when models are
 169 prompted to reason step-by-step using CoT, test-time strategies have room to work. This setup enables
 170 both feature-based (e.g., CoT length, pivot words) and confidence-based (e.g., MV) approaches.

171 As shown in Fig. 1 (right), MV consistently improves performance across all benchmarks, with
 172 average gains of 2-4%. This validates the utility of test-time sampling under CoT: the model explores
 173 diverse reasoning paths and occasionally corrects itself. However, the improvements are modest,
 174 suggesting that sampled CoTs are still highly correlated, a hypothesis we will formally investigate
 175 in § 4. Meanwhile, feature-based methods fail to provide any consistent gain over vanilla CoT.
 176 Their performance often fluctuates slightly around the baseline. This highlights a key difference
 177 from LLMs: in VLMs, textual heuristics are poor proxies for reasoning correctness because visual
 178 understanding is the bottleneck. If perception fails, even a well-formed CoT cannot save the answer.

179 **Takeaway.** TTC can improve visual reasoning, but only under specific conditions. Without CoT
 180 prompting, models produce nearly identical outputs, leaving no room for improvement. Even with
 181 CoT, gains from MV are modest, and feature-based scoring fails to help, highlighting the unique
 182 challenges of visual reasoning where perception quality limits downstream reasoning. This raises
 183 a key question: *when does TTC actually help?* To answer this, we now turn to the analysis of MV,
 184 focusing on how its effectiveness depends on the statistical dependencies among model predictions.

186 4 WHEN DOES TTC WORK IN VISUAL REASONING?

187
 188 Why does test-time compute (TTC), especially majority voting (MV), sometimes fail to improve
 189 accuracy in visual reasoning? We address this question by analyzing how the statistical dependency
 190 among model predictions influences the effectiveness of MV. To this end, we develop a theoretical
 191 framework that quantifies this relationship and support it with empirical evidence.

193 4.1 THEORETICAL INSIGHT: TTC HELPS WHEN PREDICTIONS ARE DIVERSE

194
 195 **Setup.** Consider a K -choice question with a unique correct answer $Y \in [K]$. Let $X_1, \dots, X_U \in$
 196 $[K]$ be U predictions, either from U decoding samples of a single VLM or from U different VLMs in
 197 an ensemble.² Define the correctness indicator $Z_u := \mathbb{I}\{X_u = Y\}$ and let the single-trial accuracy
 198 be $p := \mathbb{E}[Z_u]$. Let $S_k := \sum_{u=1}^U \mathbb{I}\{X_u = k\}$ denote the number of votes for option k , and let the
 199 MV prediction be $\hat{Y}_{\text{MV}} := \arg \max_k S_k$. Define the MV accuracy as $A_{\text{MV}}(U) := \mathbb{P}(\hat{Y}_{\text{MV}} = Y)$,
 200 and the improvement as $\Delta A_{\text{MV}}(U) := A_{\text{MV}}(U) - p$.

201
 202 **Dependency metrics.** To understand when MV is effective, we quantify the *dependency* among
 203 predictions using two metrics: *normalized mutual information (NMI)* and *correlation*. For answer
 204 variables X, X' , we define NMI as

$$205 \text{NMI}(X; X') := \frac{I(X; X')}{\min\{H(X), H(X')\}}, \quad H(X) = -\sum_{k=1}^K \mathbb{P}(X = k) \log \mathbb{P}(X = k).$$

208 For U predictions, the average NMI is:

$$209 \overline{\text{NMI}} := \frac{2}{U(U-1)} \sum_{u < v} \text{NMI}(X_u; X_v).$$

212 For correctness indicators Z, Z' , define the *correlation* as

$$213 \rho(Z, Z') := \frac{\mathbb{E}[ZZ'] - p^2}{p(1-p)}, \quad \bar{\rho} := \frac{2}{U(U-1)} \sum_{u < v} \rho(Z_u, Z_v).$$

215
 216 ²The theoretical result holds regardless of the origin of the U predictions.

216 **Theorem 1.** Suppose all prediction pairs (X_u, X_v) share the same dependency level (i.e., $\overline{\text{NMI}}$ or $\overline{\rho}$).
 217 Then the MV improvement $\Delta A_{\text{MV}}(U)$ is monotonically decreasing in both $\overline{\rho}$ and $\overline{\text{NMI}}$. In particular:
 218

$$\overline{\rho} = 1 \text{ (or } \overline{\text{NMI}} = 1 \Rightarrow \Delta A_{\text{MV}}(U) = 0,$$

$$\overline{\rho} = 0 \text{ (or } \overline{\text{NMI}} = 0), p > \frac{1}{K} \Rightarrow A_{\text{MV}}(U) \rightarrow 1 \text{ as } U \rightarrow \infty.$$

222 **Interpretation.** The proof is provided in App. B.1. This theorem reveals a simple but powerful
 223 insight: *MV only improves accuracy when predictions are diverse*. If all predictions are identical
 224 (i.e., fully dependent), MV reduces to a single prediction, yielding no gain. But if predictions are
 225 uncorrelated and individually better than random guessing ($p > 1/K$), MV can aggregate signal and
 226 achieve near-perfect accuracy as the number of predictions U grows. Both $\overline{\rho}$ and $\overline{\text{NMI}}$ are practical,
 227 interpretable, and model-agnostic indicators of this diversity. Thus, they can serve as useful tools to
 228 estimate when TTC is likely to help, without relying on ground truth labels or model internals.
 229

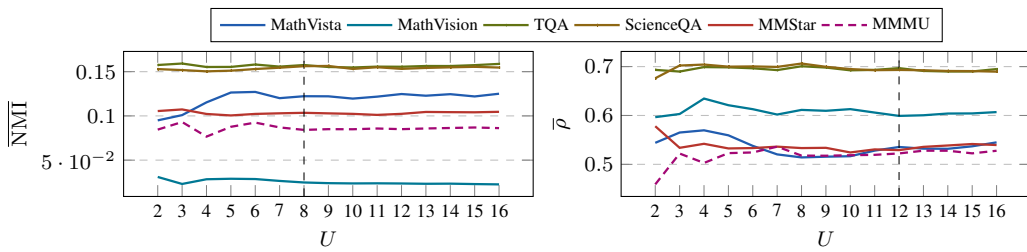
230 4.2 EMPIRICAL VERIFICATION

231 We now provide empirical evidence to support our theoretical findings in § 4.1. In particular, we
 232 examine how model prediction dependency, quantified by $\overline{\text{NMI}}$ and $\overline{\rho}$, affects MV performance.
 233 Our goal is twofold: (1) determine how many decoding samples U are sufficient to obtain stable
 234 dependency estimates and maximal MV improvement, and (2) empirically verify the theoretical
 235 prediction that MV improvement decreases with increasing dependency.
 236

237 4.2.1 HOW MANY DECODING SAMPLES ARE SUFFICIENT?

238 Our theoretical analysis assumes a sufficiently large number of decoding samples U , such that MV
 239 benefits fully materialize. In practice, however, increasing U incurs additional computational cost.
 240 Thus, we first investigate the convergence of dependency metrics as U grows, aiming to find the
 241 minimal U that yields stable estimates.
 242

243 **Setup.** We use Qwen-7B to generate $U = 2$ to 16 decoded outputs for each example across six
 244 visual reasoning datasets. For each U , we compute two dependency metrics: average normalized
 245 mutual information $\overline{\text{NMI}}$ and average correctness correlation $\overline{\rho}$ between response pairs.
 246



255 Figure 2: Convergence of dependency with decoding sample size U on Qwen-7B. Both $\overline{\text{NMI}}$ and $\overline{\rho}$ stabilize
 256 when $U=12$, suggesting that a moderate number of samples is sufficient to estimate dependency reliably.
 257

258 **Findings.** As shown in Fig. 2, both $\overline{\text{NMI}}$ and $\overline{\rho}$ stabilize around $U = 12$ across all datasets. Beyond
 259 this point, additional samples offer minimal benefit in estimating prediction dependency. Sampling
 260 more than 12 responses provides diminishing returns in estimating dependency. Thus, we use $U = 16$
 261 in all subsequent experiments to ensure both stability and tractability.
 262

263 4.2.2 DOES MV IMPROVEMENT DECREASE WITH DEPENDENCY?

265 Next, we test our core theoretical prediction: MV is most beneficial when model outputs are diverse.
 266 That is, MV improvement should decrease as prediction dependency increases.
 267

268 **Setup.** We evaluate MV improvement $\Delta A_{\text{MV}}(16)$ for seven models across six datasets, using
 269 $U = 16$ decoding samples. For each model, we compute the average improvement and average
 dependency across datasets, measuring dependency with both $\overline{\text{NMI}}$ and $\overline{\rho}$.

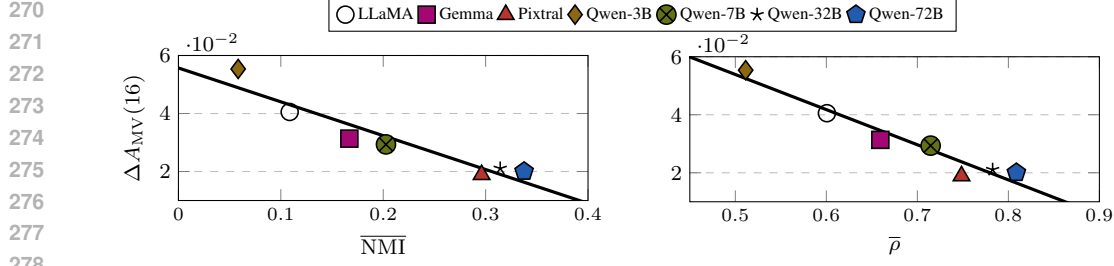


Figure 3: MV improvement decreases with higher prediction dependency. Across models, MV improvement $\Delta A_{MV}(16)$ is negatively correlated with both \overline{NMI} and $\bar{\rho}$, confirming theoretical predictions.

Findings. Fig. 3 shows a clear negative correlation between MV improvement and both dependency metrics. Smaller models (e.g., Qwen-3B, LLaMA), which produce more diverse outputs, benefit more from MV. In contrast, larger or more deterministic models (e.g., Qwen-72B, Pixtral) exhibit limited diversity and gain less from MV. Detailed results are in Figs. 6 and 7 in App. D.1.

Takeaway. MV effectiveness hinges on the diversity of model outputs. As predictions become more deterministic, reflected by higher dependency metrics such as \overline{NMI} and $\bar{\rho}$, MV offers diminishing returns. This empirical trend aligns with our theoretical findings and suggests a practical principle: MV is most beneficial when applied to weaker or smaller models, or in settings where the model’s confidence is low and outputs are more stochastic. For example, in few-shot or domain-shifted scenarios where models are uncertain, decoding diversity tends to be higher, allowing MV to amplify weak but complementary signals. Conversely, when using large, over-optimized models that produce highly consistent predictions (e.g., Qwen-72B), MV is unlikely to help and may introduce unnecessary compute cost. Overall, this analysis provides a practical lens for when and why to apply TTC strategies like MV in real-world visual reasoning tasks.

5 BEYOND MV: ENTROPY-BASED TTC FOR MULTI-MODEL ENSEMBLES

Building on the insight that MV benefits from diverse yet independent predictions, we now turn to the more realistic and underexplored *multi-model ensemble* setting. Compared to multi-round decoding from a single model, where prediction diversity is limited, ensembles of heterogeneous models naturally offer complementary strengths and errors. Here, we first introduce an entropy-based TTC method (ETTC) designed to better leverage cross-model diversity. We then theoretically show that ETTC outperforms MV under mild conditions, and empirically demonstrate that it enables smaller models to enhance or even surpass larger ones in visual reasoning.

5.1 ENTROPY-BASED TTC (ETTC)

Our previous analysis showed that the effectiveness of MV depends heavily on prediction diversity. However, MV has a deeper limitation in multi-model ensemble settings: it assumes all model responses are equally reliable and votes based solely on frequency, ignoring how confident or capable each model is. This oversight is less problematic in the single-model setting, since all predictions come from the same model, their expected quality is the same. But in multi-model ensembles, where models vary in size, training, and performance, this uniform treatment becomes a liability. A majority of weaker models can outvote a stronger one, even when the latter is confidently correct.

To address this, we introduce Entropy-Based Test-Time Compute (ETTC): a simple, model-agnostic method that selects the most confident prediction among multiple sources, rather than relying on vote counts. ETTC uses normalized predictive entropy as a proxy for confidence.

Definition 1 (Entropy-Based Selection Rule). *Let U sources (models or decoding rounds) each produce a predictive distribution $p_u(\cdot) \in \Delta^{K-1}$ over K answer options. Define the normalized entropy as*

$$\tilde{H}_u := -\frac{1}{\log K} \sum_{k=1}^K p_u(k) \log p_u(k) \in [0, 1],$$

324 and the top-1 prediction $\hat{y}_u := \arg \max_k p_u(k)$. ETTC selects the least-uncertain source,
 325

$$326 \quad u^* := \arg \min_{u \in [U]} \tilde{H}_u, \quad \hat{Y}_{\min H} := \hat{y}_{u^*}. \\ 327$$

328 This selection rule prioritizes predictions with lower uncertainty, under the intuition that higher
 329 model confidence often correlates with correctness, especially for well-calibrated or stronger models.
 330 In contrast to MV, which can amplify weak or erroneous signals through majority effects, ETTC
 331 amplifies precision by trusting the most decisive prediction. Notably, ETTC reduces to MV in the
 332 single-model multi-round case when we average predictive distributions and pick the most probable
 333 option. But in the multi-model setting, it diverges: it allows stronger models to dominate the decision,
 334 even when they are in the minority, an essential property for leveraging heterogeneous ensembles.
 335

336 **Takeaway.** ETTC replaces vote count with model confidence, providing a more principled and
 337 adaptive aggregation strategy for ensemble reasoning. Especially in real-world scenarios where
 338 model capabilities vary, ETTC is better equipped to avoid over-reliance on weaker models and better
 339 exploit the reliability of stronger ones.
 340

5.2 THEORETICAL INSIGHT: ETTC OUTPERFORMS MV IN MULTI-MODEL ENSEMBLES

342 In the multi-model ensemble setting, models vary in strength and reliability, which increases the
 343 answer diversity. While MV treats models equally, this can backfire: weaker models may collectively
 344 outvote stronger ones, especially when their errors are correlated. Our goal is to theoretically
 345 understand why the proposed ETTC method provides a more robust alternative in such scenarios.
 346

347 We begin by formalizing a key intuition: *more confident predictions tend to be more accurate.*
 348

349 **Assumption 1** (Entropy-Accuracy Monotonicity). *For a given input with true label Y , suppose
 350 model u assigns probability $p_u(Y)$ to Y , and \tilde{H}_u is its normalized entropy. Then, for all $u, v \in [U]$:*

$$351 \quad p_u(Y) > p_v(Y) \Rightarrow \tilde{H}_u < \tilde{H}_v.$$

352 This assumption states that a model assigning a higher probability to the correct answer also tends to
 353 be more confident (i.e., has lower entropy). While this relationship may not hold perfectly, we find
 354 that it holds approximately in practice across datasets and models (see Fig. 8 in App. D.2).
 355

356 Given this, ETTC simply selects the prediction from the most confident model (i.e., with lowest
 357 entropy on the answer distribution). Let $c^* := \Pr(\hat{y}_{u^*} = Y)$ be the accuracy of the most accurate
 358 model u^* . ETTC guarantees performance at least c^* , and may occasionally do better by selecting
 359 another model whose prediction is both confident and correct. To model dependency among models,
 360 we consider a simple coupling scheme: with probability λ , all non-best models copy the same
 361 prediction W (e.g., due to shared biases or training data); with probability $1 - \lambda$, their predictions
 362 are conditionally independent. Let $\bar{c} := \Pr(W = Y)$ be the accuracy of this “bloc” prediction, and
 $A_{\text{MV}}(0)$ be the MV accuracy in the fully independent case.
 363

Theorem 2 (Superiority of ETTC over MV). *With the setup above and under Assumption 1, let
 364 $A_{\min H} := \Pr(\hat{y}_{\min H} = Y)$ be the ETTC accuracy. Then for all $\lambda \in [0, 1]$, we have:*

$$365 \quad A_{\text{MV}}(\lambda) = \lambda \bar{c} + (1 - \lambda) A_{\text{MV}}(0), \quad (1)$$

$$366 \quad A_{\min H} - A_{\text{MV}}(\lambda) = \lambda(c^* - \bar{c}) + (1 - \lambda)(A_{\min H} - A_{\text{MV}}(0)). \quad (2)$$

367 In particular, $A_{\min H} \geq A_{\text{MV}}(\lambda)$ for all λ , with strict inequality whenever $\lambda > 0$ and $\bar{c} < c^*$.
 368

369 **Interpretation.** The proof is in App. B.2. This result highlights a fundamental difference between
 370 ETTC and MV in multi-model ensembles. MV aggregates predictions without considering model
 371 quality, making it vulnerable to correlated errors, especially when several weaker models dominate
 372 the vote. As the error correlation increases (i.e., higher λ), MV accuracy degrades and converges to
 373 that of the bloc prediction \bar{c} , which may be substantially lower than the best model’s accuracy c^* . In
 374 contrast, ETTC avoids this failure mode by selecting the most confident prediction. Under a mild
 375 assumption that lower entropy correlates with higher accuracy, ETTC guarantees performance at
 376 least as good as the most accurate model, and can even exceed it in practice. Since VLMs often share
 377 training data or architecture, making their predictions dependent, ETTC offers a more robust and
 378 principled strategy for test-time inference in ensemble settings.
 379

378 5.3 EMPIRICAL VERIFICATION
379380 We now evaluate ETTC in practical multi-model ensemble settings and compare its performance to
381 MV. While our theory highlights ETTC’s robustness under dependency, here we empirically verify
382 its effectiveness across two representative ensemble configurations: (1) diverse models of similar size
383 from different families, and (2) scaled models within the same architecture family.384
385 5.3.1 SIMILAR-SIZED MODELS FROM DIFFERENT FAMILIES
386387 This experiment evaluates whether ETTC can better leverage diversity among models of comparable
388 size but distinct families. In this setting, models differ in architecture, training data, and accuracy,
389 offering complementary strengths, but also potential variance in prediction quality and confidence.390 **Setup.** We select four models of similar scale (7B-12B): LLaMA, Pixtral, Gemma, and Qwen-7B.
391 These models produce predictions for each dataset, and we compare MV and ETTC on the same set
392 of outputs. Notably, no single model consistently dominates across all tasks, and some (e.g., LLaMA)
393 are clearly weaker, adding noise to aggregation.394
395 Table 1: Comparison of ETTC and MV in the multi-model ensemble setting with *similar-sized models from*
396 *different families*. ETTC consistently outperforms MV across all six datasets, with particularly large gains on
397 benchmarks where model accuracies vary widely (e.g., MathVista, MathVision). This highlights ETTC’s ability
398 to prioritize stronger models when aggregating predictions.

| 400 401 402 403 404 405 406 407 408 409 410 411 412 413 414 415 416 417 418 419 420 421 422 423 424 425 426 427 428 429 430 431 | | 400 401 402 403 404 405 406 407 408 409 410 411 412 413 414 415 416 417 418 419 420 421 422 423 424 425 426 427 428 429 430 431 | | | | Average | MV | ETTC |
|------------------------------------------------------------------------------------------------------------------------------------------------------------------------------------------------------------------------------|-------|------------------------------------------------------------------------------------------------------------------------------------------------------------------------------------------------------------------------------|---------|-------|---------|------------------------------------------------------------------------------------------------------------------------------------------------------------------------------------------------------------------------------|--------------|------|
| 400 401 402 403 404 405 406 407 408 409 410 411 412 413 414 415 416 417 418 419 420 421 422 423 424 425 426 427 428 429 430 431 | | LLaMA | Pixtral | Gemma | Qwen-7B | 400 401 402 403 404 405 406 407 408 409 410 411 412 413 414 415 416 417 418 419 420 421 422 423 424 425 426 427 428 429 430 431 | | |
| MathVista | 52.04 | 56.03 | 65.03 | 72.08 | 61.30 | 68.33 | 75.93 | |
| MathVision | 23.41 | 25.20 | 31.84 | 30.18 | 27.66 | <u>32.05</u> | 35.57 | |
| TQA | 70.41 | 77.34 | 78.86 | 78.50 | 76.28 | <u>83.65</u> | 83.90 | |
| ScienceQA | 77.84 | 78.32 | 77.83 | 79.76 | 78.44 | 85.52 | <u>85.28</u> | |
| MMStar | 46.09 | 50.35 | 53.40 | 56.77 | 51.65 | <u>59.27</u> | 60.07 | |
| MMMU | 42.87 | 47.65 | 52.49 | 50.53 | 48.39 | <u>53.66</u> | 58.63 | |
| Average | 52.11 | 55.82 | 59.91 | 61.30 | 57.29 | <u>63.75</u> | 66.56 | |

411 **Findings.** As shown in Tab. 1, ETTC outperforms MV on five of six datasets, with an average
412 accuracy gain of +2.81% (66.56% vs. 63.75%). Larger improvements are seen on tasks where model
413 performance diverges significantly, such as MathVista and MathVision. In these cases, MV suffers
414 from equal-weighting all predictions, allowing weaker models to dilute the ensemble’s signal. In
415 contrast, ETTC adaptively prioritizes high-confidence predictions, often aligning with the stronger
416 model per item, and in some cases even exceeding the best model’s standalone performance.417 **Takeaway.** When aggregating diverse but uneven models, ETTC offers a clear advantage: it
418 selectively filters noise from weaker models based on confidence, making it particularly effective in
419 heterogeneous ensemble settings where voting can be misled by inaccurate predictions.420
421 5.3.2 SAME-FAMILY MODELS OF DIFFERENT SCALES
422423 This experiment examines whether ETTC remains effective when models share the same architecture
424 and training data, but differ in scale. While such ensembles may suffer from prediction correlation
425 due to shared inductive biases, scaling laws suggest that performance gaps between model sizes can
426 still introduce meaningful diversity into their predictions.427 **Setup.** We use four models from the Qwen family: 3B, 7B, 32B, and 72B. Each model produces
428 predictions on all datasets, and we compare MV and ETTC on their combined outputs. Since all
429 models come from the same training pipeline, this setting represents a high-dependency ensemble,
430 posing a challenge for MV. However, scaling-induced performance gaps can create asymmetric
431 confidence signals that ETTC may exploit.

432 Table 2: Comparison of ETTC and MV in the multi-model ensemble setting using *same-family models* (Qwen)
 433 of increasing scale. ETTC consistently outperforms MV across all datasets, even under highly correlated
 434 predictions. Gains are especially pronounced when model accuracies increase with scale, demonstrating ETTC’s
 435 advantage in prioritizing stronger models within homogeneous ensembles.

| Accuracy (%) | Models | | | | Average | MV | ETTC |
|----------------|---------|---------|----------|--------------|---------|--------------|--------------|
| | Qwen-3B | Qwen-7B | Qwen-32B | Qwen-72B | | | |
| MathVista | 51.94 | 72.08 | 78.58 | 80.58 | 70.80 | <u>83.15</u> | 84.44 |
| MathVision | 22.27 | 30.18 | 38.80 | <u>42.89</u> | 33.53 | 41.32 | 44.84 |
| TQA | 60.85 | 78.50 | 83.06 | <u>84.52</u> | 76.73 | <u>84.90</u> | 86.70 |
| ScienceQA | 66.67 | 79.76 | 84.21 | <u>84.64</u> | 78.82 | 84.04 | 85.03 |
| MMStar | 41.22 | 56.77 | 56.34 | <u>62.56</u> | 54.22 | 61.00 | 63.73 |
| MMMU | 37.41 | 50.53 | 59.04 | <u>64.18</u> | 52.79 | 58.63 | 65.34 |
| Average | 46.73 | 61.30 | 66.67 | <u>69.90</u> | 61.15 | 68.84 | 71.68 |

448 **Findings** As shown in Tab. 2, ETTC outperforms MV on all datasets, achieving an average gain of
 449 $+2.84\%$ (71.68% vs. 68.84%). While overall prediction correlation is higher than in the cross-family
 450 setting, the performance variance introduced by scale still provides useful diversity, particularly
 451 when smaller models make correct predictions with higher certainty than their larger counterparts.
 452 ETTC is able to detect and leverage these instances, occasionally selecting smaller models to override
 453 incorrect large-model predictions. In general, ETTC surpasses the accuracy of the strongest model
 454 (Qwen-72B) while MV sometimes provides worse performance compared to the strongest model.
 455 This show the ability of ETTC to dynamically integrate strengths across the scale spectrum.

456 **Takeaway.** Despite architectural homogeneity, ensembles of different-sized models still benefit
 457 from confidence-based selection. ETTC not only avoids overcounting correlated errors but also
 458 allows smaller models to meaningfully enhance or correct the outputs of larger ones, challenging
 459 the conventional wisdom that bigger models alone should dominate in test-time ensembles. This
 460 highlights ETTC’s potential as a lightweight, plug-and-play strategy for amplifying large model
 461 performance with smaller, cheaper components.

463 **Overall Summary.** Across both ensemble settings, diverse and redundant, ETTC consistently
 464 outperforms MV without requiring additional training or tuning. These results empirically confirm
 465 our theoretical findings: when dependency undermines voting, entropy-based selection offers a more
 466 robust and adaptive path to test-time improvement in visual reasoning tasks.

468 **Supervised Variant of ETTC.** We further extend ETTC to a supervised variant that learns to
 469 calibrate confidence signals based on past correctness (App. D.3). We show that even a lightweight
 470 classifier trained with minimal supervision significantly improves performance over (unsupervised)
 471 ETTC. This suggests that combining confidence with supervised trust modeling offers a promising
 472 direction for more adaptive test-time strategies.

475 6 CONCLUSION

477 We present a comprehensive study of test-time compute (TTC) strategies for visual reasoning,
 478 focusing on when and how repeated inference can improve accuracy. Our theoretical and empirical
 479 analyses reveal that the effectiveness of majority voting (MV) is tightly linked to the diversity and
 480 independence of predictions. While MV offers gains in low-dependency regimes, it fails when
 481 outputs are correlated or dominated by weak models. To address these limitations, we propose
 482 ETTC: an entropy-based method that selects the most confident prediction, along with a supervised
 483 variant that learns when low-entropy signals are reliable. Both methods consistently outperform MV
 484 across settings, enabling smaller models to boost larger ones in multi-model ensembles. Our findings
 485 highlight confidence, not frequency, as the key to robust TTC in visual reasoning, and offer simple,
 scalable methods for improving performance without retraining or fine-tuning.

486 ETHICS STATEMENT
487488 This work does not involve human subjects, sensitive data, or potentially harmful applications.
489 All datasets used are publicly available and widely adopted in the vision-language and reasoning
490 communities. We follow best practices in data handling, model evaluation, and reproducibility, and
491 adhere to the ICLR Code of Ethics in all aspects of our research.
492493 REPRODUCIBILITY STATEMENT
494495 We provide all necessary details to ensure the reproducibility of our work. Model descriptions,
496 experimental setups, and theoretical assumptions are described in the main text and appendix.
497 Complete proofs of theoretical results are provided in App. B. Code and evaluation scripts will be
498 released publicly upon publication.
499500 REFERENCES
501

502 Pravesh Agrawal, Szymon Antoniak, Emma Bou Hanna, Baptiste Bout, Devendra Singh Chaplot,
503 Jessica Chudnovsky, Diogo Costa, Baudouin De Monicault, Saurabh Garg, Théophile Gervet,
504 Soham Ghosh, Amélie Héliou, Paul Jacob, Albert Q. Jiang, Kartik Khandelwal, Timothée Lacroix,
505 Guillaume Lample, Diego de Las Casas, Thibaut Lavril, Teven Le Scao, Andy Lo, William
506 Marshall, Louis Martin, Arthur Mensch, Pavankumar Muddireddy, Valera Nemychnikova, Marie
507 Pellat, Patrick von Platen, Nikhil Raghuraman, Baptiste Rozière, Alexandre Sablayrolles, Lucile
508 Saulnier, Romain Sauvestre, Wendy Shang, Roman Soletskyi, Lawrence Stewart, Pierre Stock,
509 Joachim Studnia, Sandeep Subramanian, Sagar Vaze, Thomas Wang, and Sophia Yang. Pixtral
510 12b. *CoRR*, abs/2410.07073, 2024. doi: 10.48550/ARXIV.2410.07073. URL <https://doi.org/10.48550/arXiv.2410.07073>.
511

512 Haider Al-Tahan, Quentin Garrido, Randall Balestrieri, Diane Bouchacourt, Caner Hazirbas, and
513 Mark Ibrahim. Unibench: Visual reasoning requires rethinking vision-language beyond scaling,
514 2024. URL <https://arxiv.org/abs/2408.04810>.

515 Shuai Bai, Keqin Chen, Xuejing Liu, Jialin Wang, Wenbin Ge, Sibo Song, Kai Dang, Peng Wang,
516 Shijie Wang, Jun Tang, Humen Zhong, Yuanzhi Zhu, Ming-Hsuan Yang, Zhaohai Li, Jianqiang
517 Wan, Pengfei Wang, Wei Ding, Zheren Fu, Yiheng Xu, Jiabo Ye, Xi Zhang, Tianbao Xie, Zesen
518 Cheng, Hang Zhang, Zhibo Yang, Haiyang Xu, and Junyang Lin. Qwen2.5-vl technical report.
519 *CoRR*, abs/2502.13923, 2025. doi: 10.48550/ARXIV.2502.13923. URL <https://doi.org/10.48550/arXiv.2502.13923>.
520

521 Apratim Bhattacharyya, Sunny Panchal, Mingu Lee, Reza Pourreza, Pulkit Madan, and Roland
522 Memisevic. Look, remember and reason: Visual reasoning with grounded rationales. *CoRR*,
523 abs/2306.17778, 2023. doi: 10.48550/ARXIV.2306.17778. URL <https://doi.org/10.48550/arXiv.2306.17778>.
524

525 Edward Y. Chang, Yuxuan Tong, Morry Niu, Graham Neubig, and Xiang Yue. Demystifying long
526 chain-of-thought reasoning in llms. *CoRR*, abs/2502.03373, 2025. doi: 10.48550/ARXIV.2502.
527 03373. URL <https://doi.org/10.48550/arXiv.2502.03373>.
528

529 Lin Chen, Jinsong Li, Xiaoyi Dong, Pan Zhang, Yuhang Zang, Zehui Chen, Haodong Duan,
530 Jiaqi Wang, Yu Qiao, Dahua Lin, and Feng Zhao. Are we on the right way for eval-
531 uating large vision-language models? In Amir Globersons, Lester Mackey, Danielle Bel-
532 grave, Angela Fan, Ulrich Paquet, Jakub M. Tomczak, and Cheng Zhang (eds.), *Advances*
533 in *Neural Information Processing Systems 38: Annual Conference on Neural Infor-
534 mation Processing Systems 2024, NeurIPS 2024, Vancouver, BC, Canada, December 10 - 15,*
535 2024, 2024a. URL http://papers.nips.cc/paper_files/paper/2024/hash/2f8ee6a3d766b426d2618e555b5aeb39-Abstract-Conference.html.
536

537 Wenqing Chen, Weicheng Wang, Zhixuan Chu, Kui Ren, Zibin Zheng, and Zhichao Lu. Self-para-
538 consistency: Improving reasoning tasks at low cost for large language models. In Lun-Wei Ku,
539 Andre Martins, and Vivek Srikumar (eds.), *Findings of the Association for Computational Linguis-
tics, ACL 2024, Bangkok, Thailand and virtual meeting, August 11-16, 2024*, pp. 14162–14167.

540 Association for Computational Linguistics, 2024b. doi: 10.18653/V1/2024.FINDINGS-ACL.842.
 541 URL <https://doi.org/10.18653/v1/2024.findings-acl.842>.

542 Zhenfang Chen, Qinhong Zhou, Yikang Shen, Yining Hong, Zhiqing Sun, Dan Gutfreund, and Chuang
 543 Gan. Visual chain-of-thought prompting for knowledge-based visual reasoning. In Michael J.
 544 Wooldridge, Jennifer G. Dy, and Sriraam Natarajan (eds.), *Thirty-Eighth AAAI Conference on
 545 Artificial Intelligence, AAAI 2024, Thirty-Sixth Conference on Innovative Applications of Artificial
 546 Intelligence, IAAI 2024, Fourteenth Symposium on Educational Advances in Artificial Intelligence,
 547 EAAI 2014, February 20-27, 2024, Vancouver, Canada*, pp. 1254–1262. AAAI Press, 2024c. doi:
 548 10.1609/AAAI.V38I2.27888. URL <https://doi.org/10.1609/aaai.v38i2.27888>.

549

550 Shih-Han Chou, Shivam Chandhok, James J. Little, and Leonid Sigal. Test-time consistency in
 551 vision language models. *CoRR*, abs/2506.22395, 2025. doi: 10.48550/ARXIV.2506.22395. URL
 552 <https://doi.org/10.48550/arXiv.2506.22395>.

553 Franz Dietrich and Christian List. Probabilistic opinion pooling generalized. part two: the premise-
 554 based approach. *Soc. Choice Welf.*, 48(4):787–814, 2017. doi: 10.1007/S00355-017-1035-Y. URL
 555 <https://doi.org/10.1007/s00355-017-1035-y>.

556

557 Yao Fu, Hao Peng, Ashish Sabharwal, Peter Clark, and Tushar Khot. Complexity-based prompting for
 558 multi-step reasoning. In *The Eleventh International Conference on Learning Representations, ICLR
 559 2023, Kigali, Rwanda, May 1-5, 2023*. OpenReview.net, 2023. URL <https://openreview.net/forum?id=yflicZHC-19>.

560

561 Google Gemini Team. Gemini 2.5: Pushing the frontier with advanced reasoning, multimodality, long
 562 context, and next generation agentic capabilities, 2025. URL <https://arxiv.org/abs/2507.06261>.

563

564 Google DeepMind Gemma Team. Gemma 3 technical report. *CoRR*, abs/2503.19786, 2025. doi: 10.
 565 48550/ARXIV.2503.19786. URL <https://doi.org/10.48550/arXiv.2503.19786>.

566

567 Chuan Guo, Geoff Pleiss, Yu Sun, and Kilian Q. Weinberger. On calibration of modern neural
 568 networks. In Doina Precup and Yee Whye Teh (eds.), *Proceedings of the 34th International
 569 Conference on Machine Learning, ICML 2017, Sydney, NSW, Australia, 6-11 August 2017*, vol-
 570 ume 70 of *Proceedings of Machine Learning Research*, pp. 1321–1330. PMLR, 2017. URL
 571 <http://proceedings.mlr.press/v70/guo17a.html>.

572

573 Dongzhi Jiang, Renrui Zhang, Ziyu Guo, Yanwei Li, Yu Qi, Xinyan Chen, Liuhi Wang, Jianhan
 574 Jin, Claire Guo, Shen Yan, Bo Zhang, Chaoyou Fu, Peng Gao, and Hongsheng Li. Mme-cot:
 575 Benchmarking chain-of-thought in large multimodal models for reasoning quality, robustness,
 576 and efficiency. *CoRR*, abs/2502.09621, 2025. doi: 10.48550/ARXIV.2502.09621. URL <https://doi.org/10.48550/arXiv.2502.09621>.

577

578 Mingyu Jin, Qinkai Yu, Dong Shu, Haiyan Zhao, Wenyue Hua, Yanda Meng, Yongfeng Zhang,
 579 and Mengnan Du. The impact of reasoning step length on large language models. In Lun-Wei
 580 Ku, Andre Martins, and Vivek Srikumar (eds.), *Findings of the Association for Computational
 581 Linguistics, ACL 2024, Bangkok, Thailand and virtual meeting, August 11-16, 2024*, pp. 1830–1842.
 582 Association for Computational Linguistics, 2024. doi: 10.18653/V1/2024.FINDINGS-ACL.108.
 583 URL <https://doi.org/10.18653/v1/2024.findings-acl.108>.

584

585 Daesik Kim, Seonhoon Kim, and Nojun Kwak. Textbook question answering with multi-modal
 586 context graph understanding and self-supervised open-set comprehension. In Anna Korhonen,
 587 David R. Traum, and Lluís Márquez (eds.), *Proceedings of the 57th Conference of the Association
 588 for Computational Linguistics, ACL 2019, Florence, Italy, July 28- August 2, 2019, Volume 1:
 589 Long Papers*, pp. 3568–3584. Association for Computational Linguistics, 2019. doi: 10.18653/V1/
 P19-1347. URL <https://doi.org/10.18653/v1/p19-1347>.

590

591 Takeshi Kojima, Shixiang Shane Gu, Machel Reid, Yutaka Matsuo, and Yusuke Iwa-
 592 sawa. Large language models are zero-shot reasoners. In Sanmi Koyejo, S. Mo-
 593 hamed, A. Agarwal, Danielle Belgrave, K. Cho, and A. Oh (eds.), *Advances in Neural
 594 Information Processing Systems 35: Annual Conference on Neural Information Process-
 595 ing Systems 2022, NeurIPS 2022, New Orleans, LA, USA, November 28 - December 9,*

594 2022, 2022. URL http://papers.nips.cc/paper_files/paper/2022/hash/8bb0d291acd4acf06ef112099c16f326-Abstract-Conference.html.
 595
 596

597 Ludmila I. Kuncheva and Christopher J. Whitaker. Measures of diversity in classifier ensembles
 598 and their relationship with the ensemble accuracy. *Mach. Learn.*, 51(2):181–207, 2003. doi:
 599 10.1023/A:1022859003006. URL <https://doi.org/10.1023/A:1022859003006>.

600
 601 Balaji Lakshminarayanan, Alexander Pritzel, and Charles Blundell. Simple and scalable predic-
 602 tive uncertainty estimation using deep ensembles. In Isabelle Guyon, Ulrike von Luxburg,
 603 Samy Bengio, Hanna M. Wallach, Rob Fergus, S. V. N. Vishwanathan, and Roman Garnett
 604 (eds.), *Advances in Neural Information Processing Systems 30: Annual Conference on Neu-
 605 ral Information Processing Systems 2017, December 4-9, 2017, Long Beach, CA, USA*, pp.
 606 6402–6413, 2017. URL <https://proceedings.neurips.cc/paper/2017/hash/9ef2ed4b7fd2c810847ffa5fa85bce38-Abstract.html>.
 607
 608

608 Mingxiao Li, Na Su, Fang Qu, Zhizhou Zhong, Ziyang Chen, Yuan Li, Zhaopeng Tu, and Xiao-
 609 long Li. VISTA: enhancing vision-text alignment in mllms via cross-modal mutual infor-
 610 mation maximization. *CoRR*, abs/2505.10917, 2025. doi: 10.48550/ARXIV.2505.10917. URL
 611 <https://doi.org/10.48550/arXiv.2505.10917>.

612
 613 Philip Lippmann and Jie Yang. Style over substance: Distilled language models reason via stylistic
 614 replication. *CoRR*, abs/2504.01738, 2025. doi: 10.48550/ARXIV.2504.01738. URL <https://doi.org/10.48550/arXiv.2504.01738>.
 615
 616 AI @ Meta Llama Team. The llama 3 herd of models. *CoRR*, abs/2407.21783, 2024. doi: 10.48550/
 617 ARXIV.2407.21783. URL <https://doi.org/10.48550/arXiv.2407.21783>.

618
 619 Pan Lu, Swaroop Mishra, Tony Xia, Liang Qiu, Kai-Wei Chang, Song-Chun Zhu, Oyvind Tafjord,
 620 Peter Clark, and Ashwin Kalyan. Learn to explain: Multimodal reasoning via thought chains for
 621 science question answering. In *The 36th Conference on Neural Information Processing Systems
 (NeurIPS)*, 2022.

622
 623 Pan Lu, Hritik Bansal, Tony Xia, Jiacheng Liu, Chunyuan Li, Hannaneh Hajishirzi, Hao Cheng,
 624 Kai-Wei Chang, Michel Galley, and Jianfeng Gao. Mathvista: Evaluating mathematical reasoning
 625 of foundation models in visual contexts. In *The Twelfth International Conference on Learning
 626 Representations, ICLR 2024, Vienna, Austria, May 7-11, 2024*. OpenReview.net, 2024. URL
 627 <https://openreview.net/forum?id=KUNzEQMWU7>.
 628
 629 Zhenjiang Mao, Artem Bisliouk, Rohith Reddy Nama, and Ivan Ruchkin. Temporalizing confidence:
 630 Evaluation of chain-of-thought reasoning with signal temporal logic. *CoRR*, abs/2506.08243, 2025.
 631 doi: 10.48550/ARXIV.2506.08243. URL <https://doi.org/10.48550/arXiv.2506.08243>.
 632
 633 Prahitha Movva and Naga Harshita Marupaka. Enhancing scientific visual question answering
 634 through multimodal reasoning and ensemble modeling. In Tirthankar Ghosal, Philipp Mayr,
 635 Amanpreet Singh, Aakanksha Naik, Georg Rehm, Dayne Freitag, Dan Li, Sonja Schimmler, and
 636 Anita De Waard (eds.), *Proceedings of the Fifth Workshop on Scholarly Document Processing
 637 (SDP 2025)*, pp. 252–262, Vienna, Austria, July 2025. Association for Computational Linguistics.
 638 ISBN 979-8-89176-265-7. doi: 10.18653/v1/2025.sdp-1.23. URL <https://aclanthology.org/2025.sdp-1.23/>.
 639

640 OpenAI. GPT-4 technical report. *CoRR*, abs/2303.08774, 2023. doi: 10.48550/ARXIV.2303.08774.
 641 URL <https://doi.org/10.48550/arXiv.2303.08774>.
 642
 643 María Rufo and Carlos Pérez. Log-linear pool to combine prior distributions: A suggestion for a
 644 calibration-based approach. *Bayesian Analysis*, 7:1–28, 06 2012. doi: 10.1214/12-BA714.

645
 646 Charlie Snell, Jaehoon Lee, Kelvin Xu, and Aviral Kumar. Scaling LLM test-time compute optimally
 647 can be more effective than scaling model parameters. *CoRR*, abs/2408.03314, 2024. doi: 10.48550/
 648 ARXIV.2408.03314. URL <https://doi.org/10.48550/arXiv.2408.03314>.

648 Zhiqing Sun, Sheng Shen, Shengcao Cao, Haotian Liu, Chunyuan Li, Yikang Shen, Chuang Gan,
 649 Liangyan Gui, Yu-Xiong Wang, Yiming Yang, Kurt Keutzer, and Trevor Darrell. Aligning
 650 large multimodal models with factually augmented RLHF. In Lun-Wei Ku, Andre Martins, and
 651 Vivek Srikumar (eds.), *Findings of the Association for Computational Linguistics: ACL 2024*,
 652 pp. 13088–13110, Bangkok, Thailand, August 2024. Association for Computational Linguis-
 653 tics. doi: 10.18653/v1/2024.findings-acl.775. URL [https://aclanthology.org/2024-findings-acl.775/](https://aclanthology.org/2024-findings-acl.775).
 654

655 Ilya Sutskever, Oriol Vinyals, and Quoc V. Le. Sequence to sequence learning with neural networks.
 656 In Zoubin Ghahramani, Max Welling, Corinna Cortes, Neil D. Lawrence, and Kilian Q. Weinberger
 657 (eds.), *Advances in Neural Information Processing Systems 27: Annual Conference on Neural
 658 Information Processing Systems 2014, December 8-13 2014, Montreal, Quebec, Canada*, pp.
 659 3104–3112, 2014. URL <https://proceedings.neurips.cc/paper/2014/hash/a14ac55a4f27472c5d894ec1c3c743d2-Abstract.html>.
 660

661 Kagan Tumer and Joydeep Ghosh. Error correlation and error reduction in ensemble classifiers.
 662 *Connect. Sci.*, 8(3):385–404, 1996. doi: 10.1080/095400996116839. URL <https://doi.org/10.1080/095400996116839>.
 663

664 Jiacong Wang, Zijian Kang, Haochen Wang, Haiyong Jiang, Jiawen Li, Bohong Wu, Ya Wang,
 665 Jiao Ran, Xiao Liang, Chao Feng, and Jun Xiao. VGR: visual grounded reasoning. *CoRR*,
 666 abs/2506.11991, 2025. doi: 10.48550/ARXIV.2506.11991. URL <https://doi.org/10.48550/arXiv.2506.11991>.
 667

668 Ke Wang, Junting Pan, Weikang Shi, Zimu Lu, Houxing Ren, Aojun Zhou, Mingjie Zhan, and
 669 Hongsheng Li. Measuring multimodal mathematical reasoning with math-vision dataset. In Amir
 670 Globersons, Lester Mackey, Danielle Belgrave, Angela Fan, Ulrich Paquet, Jakub M. Tomczak, and
 671 Cheng Zhang (eds.), *Advances in Neural Information Processing Systems 38: Annual Conference
 672 on Neural Information Processing Systems 2024, NeurIPS 2024, Vancouver, BC, Canada,
 673 December 10 - 15, 2024*, 2024. URL http://papers.nips.cc/paper_files/paper/2024/hash/ad0edc7d5fa1a783f063646968b7315b-Abstract-Datasets_and_Benchmarks_Track.html.
 674

675 Xuezhi Wang, Jason Wei, Dale Schuurmans, Quoc V. Le, Ed H. Chi, Sharan Narang, Aakanksha
 676 Chowdhery, and Denny Zhou. Self-consistency improves chain of thought reasoning in language
 677 models. In *The Eleventh International Conference on Learning Representations, ICLR 2023, Kigali, Rwanda, May 1-5, 2023*. OpenReview.net, 2023. URL <https://openreview.net/forum?id=1PL1NIMMrw>.
 678

679 Jason Wei, Xuezhi Wang, Dale Schuurmans, Maarten Bosma, Brian Ichter, Fei Xia, Ed H. Chi,
 680 Quoc V. Le, and Denny Zhou. Chain-of-thought prompting elicits reasoning in large language
 681 models. In Sanmi Koyejo, S. Mohamed, A. Agarwal, Danielle Belgrave, K. Cho, and A. Oh (eds.),
 682 *Advances in Neural Information Processing Systems 35: Annual Conference on Neural Information
 683 Processing Systems 2022, NeurIPS 2022, New Orleans, LA, USA, November 28 - December
 684 9, 2022*, 2022. URL http://papers.nips.cc/paper_files/paper/2022/hash/9d5609613524ecf4f15af0f7b31abca4-Abstract-Conference.html.
 685

686 Qianqi Yan, Yue Fan, Hongquan Li, Shan Jiang, Yang Zhao, Xinze Guan, Ching-Chen Kuo, and
 687 Xin Eric Wang. Multimodal inconsistency reasoning (MMIR): A new benchmark for multimodal
 688 reasoning models. In Wanxiang Che, Joyce Nabende, Ekaterina Shutova, and Mohammad Taher
 689 Pilehvar (eds.), *Findings of the Association for Computational Linguistics, ACL 2025, Vienna,
 690 Austria, July 27 - August 1, 2025*, pp. 18829–18845. Association for Computational Linguistics,
 691 2025. URL <https://aclanthology.org/2025.findings-acl.964/>.
 692

693 Tianyu Yu, Yuan Yao, Haoye Zhang, Taiwen He, Yifeng Han, Ganqu Cui, Jinyi Hu, Zhiyuan Liu,
 694 Hai-Tao Zheng, and Maosong Sun. RLHF-V: towards trustworthy mllms via behavior alignment
 695 from fine-grained correctional human feedback. In *IEEE/CVF Conference on Computer Vision
 696 and Pattern Recognition, CVPR 2024, Seattle, WA, USA, June 16-22, 2024*, pp. 13807–13816.
 697 IEEE, 2024. doi: 10.1109/CVPR52733.2024.01310. URL <https://doi.org/10.1109/CVPR52733.2024.01310>.
 698

702 Xiang Yue, Yuansheng Ni, Tianyu Zheng, Kai Zhang, Ruoqi Liu, Ge Zhang, Samuel Stevens, Dongfu
703 Jiang, Weiming Ren, Yuxuan Sun, Cong Wei, Botao Yu, Ruibin Yuan, Renliang Sun, Ming Yin,
704 Boyuan Zheng, Zhenzhu Yang, Yibo Liu, Wenhao Huang, Huan Sun, Yu Su, and Wenhui Chen.
705 MMMU: A massive multi-discipline multimodal understanding and reasoning benchmark for
706 expert AGI. In *IEEE/CVF Conference on Computer Vision and Pattern Recognition, CVPR 2024,*
707 *Seattle, WA, USA, June 16-22, 2024*, pp. 9556–9567. IEEE, 2024. doi: 10.1109/CVPR52733.2024.
708 00913. URL <https://doi.org/10.1109/CVPR52733.2024.00913>.
709
710
711
712
713
714
715
716
717
718
719
720
721
722
723
724
725
726
727
728
729
730
731
732
733
734
735
736
737
738
739
740
741
742
743
744
745
746
747
748
749
750
751
752
753
754
755

756 A RELATED WORK
757

758 **Test-time compute and chain-of-thought in LLMs.** Chain-of-thought (CoT) prompting improves
759 multi-step reasoning in large language models (Wei et al., 2022; Kojima et al., 2022), and *self-*
760 *consistency* further boosts accuracy by sampling diverse reasoning paths and selecting the most
761 consistent answer (Wang et al., 2023). Recent work studies how to allocate *test-time compute* (TTC)
762 adaptively and optimally across inputs, showing that compute-optimal scaling of inference-time
763 strategies can rival or exceed scaling model size (Snell et al., 2024). These ideas motivate our transfer
764 of TTC from text-only LMs to VLMs.

765 **Test-time compute for VLMs and multimodal CoT.** CoT has been adapted to multimodal
766 reasoning and VQA, including *visual chain-of-thought* prompts and iterative "see-think-confirm"
767 procedures (Chen et al., 2024c). Emerging work explores *test-time consistency* objectives or
768 prompt/ensemble strategies for VLMs, indicating that inference-time aggregation can improve
769 semantic and answer-level consistency without retraining (Chou et al., 2025; Movva & Marupaka,
770 2025). Our study provides a systematic examination focused on visual multiple-choice reasoning and
771 shows when TTC helps via dependency analysis.

772 **Ensembling, uncertainty, and correlation.** Classic results link ensemble gains to *diversity* (low
773 error correlation) among members (Tumer & Ghosh, 1996; Kuncheva & Whitaker, 2003). Deep
774 ensembles effectively capture predictive uncertainty (Lakshminarayanan et al., 2017) and confidence
775 calibration remains critical when aggregating predictions (Guo et al., 2017). From a probabilistic
776 aggregation perspective, our entropy-based selection relates to confidence-weighted "opinion
777 pooling" (Rufo & Pérez, 2012; Dietrich & List, 2017), but we operate at test time with *per-item*
778 uncertainty to decide which model to trust, rather than pooling full distributions.

779 **Visual reasoning benchmarks and evaluation.** We evaluate on diverse visual reasoning datasets
780 spanning math, science/diagram, and general multimodal competence: MathVista (visual math
781 reasoning) (Lu et al., 2024), ScienceQA (multimodal science QA with explanations) (Lu et al.,
782 2022), MMMU (college-level multi-discipline reasoning) (Yue et al., 2024), and MMStar (vision-
783 indispensable evaluation) (Chen et al., 2024a). These benchmarks stress perception *and* reasoning,
784 making them suitable for analyzing when TTC helps.

785 **Reinforcement learning for multimodal reasoning.** Post-training with RL/RLHF has been ex-
786 plored to improve multimodal alignment and reasoning (Sun et al., 2024; Yu et al., 2024). Such
787 approaches typically require substantial labeled or preference data and non-trivial training budgets.
788 In contrast, our method is a *test-time* procedure; a lightweight supervised variant needs only a small
789 labeled set (e.g., 128 examples) for calibration.

790 B THEORETICAL PROOFS
791792 B.1 PROOF OF THEOREM 1
793

794 *Proof.* We provide a theoretical justification for the claim that the improvement from majority voting
795 (MV) decreases monotonically with statistical dependency among model predictions. We proceed by
796 defining a simple probabilistic coupling model that controls prediction dependency, and then analyze
797 how the expected MV accuracy varies with this dependency level.

801 B.1.1 COUPLING MODEL: COPY-OR-INDEPENDENT SAMPLING
802

803 We assume all U predictions $\{X_u\}_{u=1}^U$ are drawn from a shared coupling mechanism that depends on
804 a parameter $\lambda \in [0, 1]$: With probability λ , all predictions are identical copies of a single sample X .
805 With probability $1 - \lambda$, predictions are sampled independently from a shared categorical distribution
806 $\pi = (\pi_1, \dots, \pi_K)$ over K options. Formally, for any pair (X_u, X_v) ,

$$(X_u, X_v) \sim \begin{cases} (X, X), & \text{with probability } \lambda \\ (X', X''), & X', X'' \stackrel{\text{i.i.d.}}{\sim} \pi, \text{ with probability } 1 - \lambda \end{cases} \quad (1)$$

807 This ensures uniform pairwise dependency, controlled by λ .

810 B.1.2 LEMMA: BEHAVIOR OF DEPENDENCY METRICS UNDER COUPLING
811812 We now show that both statistical dependency metrics used in our main theorem, normalized mutual
813 information and correctness correlation, are monotonic in λ under this coupling.
814815 **(a) Normalized Mutual Information.** Let X, X' be two predictions drawn according to the
816 coupling in equation 1. Their joint distribution is
817

818
$$P_\lambda(i, j) = \lambda \cdot \pi_i \cdot \delta_{ij} + (1 - \lambda) \cdot \pi_i \cdot \pi_j,$$

819 where δ_{ij} is the Kronecker delta. The marginal distributions remain unchanged as π .
820821 Since mutual information $I(X; X')$ increases with λ (via the convexity of KL divergence), and the
822 marginals are fixed, the normalized mutual information $\text{NMI}(X; X')$ is also non-decreasing in λ :
823

824
$$\text{NMI}(X; X') = \frac{I(X; X')}{H(X)} \uparrow \text{ as } \lambda \uparrow.$$

825 Hence, the average pairwise NMI $\overline{\text{NMI}}$ is also monotonic in λ .
826827 **(b) Correctness Correlation.** Let $Z_u = \mathbb{I}\{X_u = Y\}$, where Y is the correct option. Denote
828 single-trial accuracy as $p = \mathbb{P}(X_u = Y)$. Then for any pair (Z_u, Z_v) : Under the “copy” case:
829 $\mathbb{P}(Z_u = Z_v = 1) = p$. Under the “independent” case: $\mathbb{P}(Z_u = Z_v = 1) = p^2$.
830831 Therefore, the covariance is
832

833
$$\text{Cov}(Z_u, Z_v) = \mathbb{E}[Z_u Z_v] - p^2 = \lambda(p - p^2) = \lambda p(1 - p),$$

834 and the correlation is
835

836
$$\rho(Z_u, Z_v) = \frac{\text{Cov}(Z_u, Z_v)}{p(1 - p)} = \lambda. \quad (2)$$

837 Thus, the average correlation $\bar{\rho} = \lambda$.
838

839 B.1.3 MAIN PROOF: MONOTONICITY OF MV IMPROVEMENT

840 Let $A_{\text{MV}}(U; \lambda)$ be the expected MV accuracy under dependency level λ , and let $A_{\text{single}} = p$ be the
841 single-trial accuracy.
842843 We decompose MV accuracy by conditioning on the latent sampling regime:
844

845
$$A_{\text{MV}}(U; \lambda) = \lambda \cdot A_{\text{MV}}(U; \text{copy}) + (1 - \lambda) \cdot A_{\text{MV}}(U; \text{iid}). \quad (3)$$

846 In the “copy” case, all predictions are identical, so MV is equivalent to a single trial: $A_{\text{MV}}(U; \text{copy}) =$
847 p . In the “iid” case, predictions are independent, and MV aggregates U samples from π ; here, accuracy
848 improves with U , approaching 1 as $U \rightarrow \infty$ if $p > \frac{1}{K}$. Thus:
849

850
$$A_{\text{MV}}(U; \lambda) = \lambda p + (1 - \lambda) A_{\text{MV}}(U; 0), \quad (4)$$

851
$$\Delta A_{\text{MV}}(U; \lambda) := A_{\text{MV}}(U; \lambda) - p = (1 - \lambda)(A_{\text{MV}}(U; 0) - p). \quad (5)$$

852 The improvement $\Delta A_{\text{MV}}(U; \lambda)$ is thus a linear function decreasing in λ , and since $\lambda = \bar{\rho}$ (from
853 equation 2) and $\overline{\text{NMI}}$ increases with λ , MV improvement is monotonically decreasing in both.
854855 B.1.4 COROLLARY (EXTREMES)
856857 If $\lambda = 1$ (i.e., $\bar{\rho} = 1$ or $\overline{\text{NMI}} = 1$), then all predictions are identical and MV offers no improvement:
858

859
$$\Delta A_{\text{MV}}(U) = 0.$$

860 If $\lambda = 0$ (i.e., predictions are independent) and $p > \frac{1}{K}$, then:
861

862
$$A_{\text{MV}}(U) \rightarrow 1 \quad \text{as} \quad U \rightarrow \infty.$$

863 \square

864 B.1.5 DISCUSSION
865

866 This result formalizes an intuitive principle: confidence-based aggregation (e.g., MV) helps only when
867 predictions are sufficiently diverse. High dependency, measured either via correctness correlation or
868 mutual information, reduces the effective information gain from additional samples. Empirical results
869 confirm this trend across VLMs and datasets: MV yields larger gains when dependency is low.

870 B.2 PROOF OF THEOREM 2
871

872 *Proof. Setup.* Fix a K -way classification item with true label Y . Let $u^* := \arg \max_u p_u(Y)$ be the
873 best model and define $c^* := \Pr(\hat{y}_{u^*} = Y)$. Let $\mathcal{B} = \{u \neq u^*\}$ be the set of non-best models, with
874 $|\mathcal{B}| \geq 2$.

875 **Coupling among non-best models.** Introduce a latent variable $L \in \{\text{copy, iid}\}$: - With probability
876 λ , $L = \text{copy}$ and all non-best models predict a shared label W ; define $\bar{c} := \Pr(W = Y)$. - With
877 probability $1 - \lambda$, $L = \text{iid}$ and the non-best predictions are drawn independently.

878 **Step 1: Accuracy of ETTC.** Under Assumption 1, ETTC selects \hat{y}_{u^*} , so:

$$879 A_{\min H} = \Pr(\hat{y}_{u^*} = Y) = c^*. \quad (6)$$

882 **Step 2: Accuracy of MV.** By law of total probability:

$$884 A_{\text{MV}}(\lambda) = \lambda \Pr(\hat{Y}_{\text{MV}} = Y \mid L = \text{copy}) + (1 - \lambda) A_{\text{MV}}(0). \quad (7)$$

885 Under $L = \text{copy}$, all non-best models predict W , forming a majority:

$$887 \Pr(\hat{Y}_{\text{MV}} = Y \mid L = \text{copy}) = \Pr(W = Y) = \bar{c}. \quad (8)$$

888 Plugging into equation 7, we recover:

$$889 A_{\text{MV}}(\lambda) = \lambda \bar{c} + (1 - \lambda) A_{\text{MV}}(0). \quad (9)$$

891 **Step 3: Difference and monotonicity.** Subtracting equation 9 from equation 6:

$$893 A_{\min H} - A_{\text{MV}}(\lambda) = \lambda(c^* - \bar{c}) + (1 - \lambda)(c^* - A_{\text{MV}}(0)). \quad (10)$$

894 This gap is nondecreasing in λ :

$$896 \frac{d}{d\lambda}(A_{\min H} - A_{\text{MV}}(\lambda)) = A_{\text{MV}}(0) - \bar{c} \geq 0.$$

898 **Step 4: Dominance threshold.** Let

$$900 \lambda^* = \max \left\{ 0, \frac{A_{\text{MV}}(0) - c^*}{A_{\text{MV}}(0) - \bar{c}} \right\}.$$

902 Then for all $\lambda \geq \lambda^*$, ETTC outperforms MV; if $\bar{c} < c^*$ and $\lambda > \lambda^*$, the gap is strict. \square

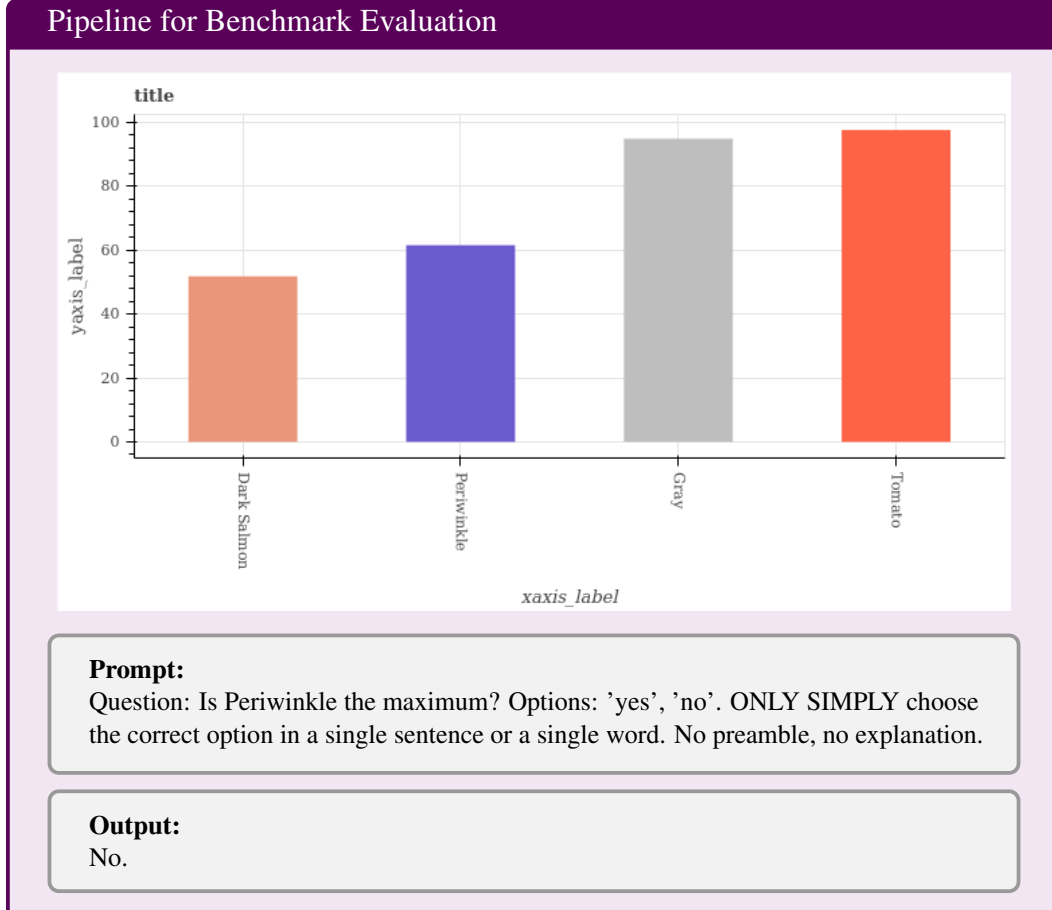
904 **Remarks.** - Since u^* is the best model, typically $\bar{c} < c^*$ unless all models perform equally well.
905 - If $A_{\text{MV}}(0) \leq c^*$, then $\lambda^* = 0$: ETTC dominates MV at all dependency levels. - Under the
906 copy-or-independent model, the average correctness correlation among non-best models equals λ
907 (see App. B.1), providing a direct link between dependency and the TTC advantage.

909 C EXPERIMENT SETTINGS
910911 C.1 DATASET
912

913 We evaluate our methods on six diverse multi-choice benchmarks spanning three domains: mathematical
914 reasoning (MathVista, MathVision), diagram-based QA (TQA, ScienceQA), and general
915 visual understanding (MMStar, MMMU). Tab. 3 summarizes key statistics, including dataset size,
916 official split used, and number of answer options. Note that some datasets contain variable numbers
917 of options (e.g., 2 - 9 in MMMU), which adds to the challenge and makes majority voting less stable.
918 This diversity ensures our evaluation reflects a wide range of real-world reasoning settings.

918
 919 Table 3: Dataset statistics and characteristics used in our evaluation. Each dataset is categorized by its domain
 920 (Math, Diagram, or General), the evaluation split used (e.g., test or validation), the number of multiple-choice
 921 questions (**Size**), and the number of answer options per question (**Option Num.**).
 922
 923
 924
 925
 926
 927
 928
 929

| Dataset | Domain | Type | Size | Option Num. |
|------------|---------|----------|-------|-------------|
| MathVista | Math | testmini | 540 | 2–8 |
| MathVision | Math | test | 1,532 | 5 |
| TQA | Diagram | test | 3,285 | 4 |
| ScienceQA | Diagram | test | 2,017 | 2–5 |
| MMStar | General | val | 1,500 | 4 |
| MMMU | General | val | 805 | 2–9 |



C.2 PROMPT

968 To ensure consistency and minimize response variance across models, we standardize the prompting
 969 format in all benchmark evaluations. Specifically, we use a direct QA prompt without explanation,
 970 and a chain-of-thought (CoT) style prompt when evaluating reasoning performance or conducting
 971 consistency analysis. Below, we show two representative examples for comparison. The image and
 972 question are kept identical, while only the prompt template changes.

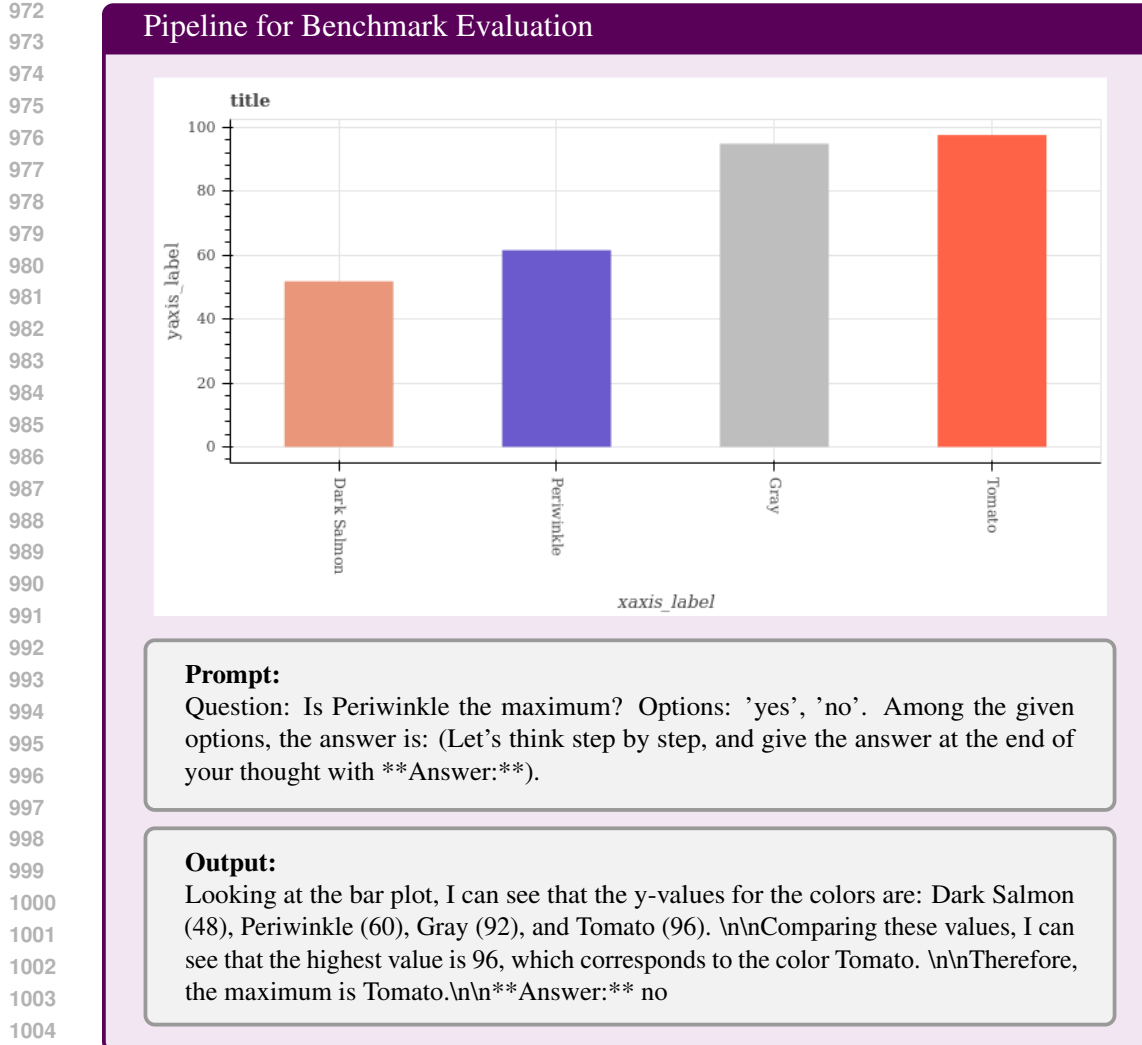


Figure 5: Example of a chain-of-thought (CoT) prompt used to elicit intermediate reasoning steps. This format is used when analyzing consistency or measuring correctness under step-by-step reasoning.

C.3 BASELINES

To better assess the reliability of CoT responses, we include several shallow feature-based baselines. These models predict the correctness of a response using surface-level properties, without access to model internals or gradient signals.

Table 4: Pivot phrases categorized by reasoning function.

| Reasoning Type | Example Phrases |
|---------------------|-------------------------------------------------------------------|
| Realization | “wait”, “oh”, “actually”, “I missed something” |
| Verification | “let me doublecheck”, “to verify”, “checking again” |
| Exploration | “what if”, “another way to look at this”, “alternatively” |
| Integration | “now I see how”, “this connects back to”, “putting this together” |

Pivot words. Pivot words are rhetorical expressions that signal shifts in reasoning, such as realization, verification, or synthesis. Prior work (Lippmann & Yang, 2025) suggests that the presence of such expressions often correlates with more deliberate and structured reasoning. We use a curated list of phrases categorized by rhetorical function, shown in Tab. 4. These are used as features for correctness prediction (e.g., counting their presence in CoTs).

Table 5: Vague expressions used in model reasoning, grouped by rhetorical effect.

| Reasoning Type | Example Phrases |
|--------------------|--------------------------------------------------------------------------------|
| Uncertainty | “maybe”, “possibly”, “perhaps”, “probably”, “might be”, “could be”, “it seems” |
| Hedging | “somewhat”, “rather”, “kind of”, “sort of”, “generally”, “typically” |

Vague words. Vague expressions are often used to hedge or express uncertainty, and may correlate with lower confidence or correctness in model reasoning. We group these into two categories, uncertainty and hedging—based on their rhetorical function. See Tab. 5.

Table 6: Overview of lexical and stylistic features used for CoT-based prediction.

| Feature | Modeling Method |
|--------------------------|----------------------------------------------------------------------------------------------------------------------------------------------------------------------------------------------|
| Token Number | Measures the number of tokens in the CoT response. Longer responses may indicate more reasoning steps, though excessive length may signal loops or noise. We vectorize it as 1/Token Number. |
| Lexical Diversity | Captures vocabulary richness by counting the number of unique tokens. Low diversity often suggests repetition. We vectorize it as 1/Vocabulary Size. |
| Pivot Word Number | Counts the number of pivot expressions from Tab. 4, indicating structured reasoning or correction. We vectorize it as 1/Pivot Word Number. |
| Vague Word Number | Counts the number of vague phrases from Tab. 5, which may reflect uncertainty or low confidence. We vectorize it as 1 – 1/Vague Word Number. |

Feature-All. We also define a feature set that combines lexical and stylistic signals for each CoT response. Specifically, we consider four interpretable features: response length (token count), lexical diversity (unique token count), number of pivot words, and number of vague words. See Tab. 6 for detailed definitions. For prediction, we compute the sum of these feature values for each example, encouraging longer, more expressive, and more structured responses, while penalizing vague expressions. The model response with the highest total score is selected as the final prediction.

D SUPPLEMENTARY RESULTS

D.1 MV IMPROVEMENT VS. \overline{NMI} AND CORRELATION

While the overall trends in Figs. 6 and 7 are consistent with our theoretical expectations, MathVision stands out as an exception. Specifically, we observe weaker or even inverted correlation between prediction dependency and MV improvement on this dataset. A likely explanation is that MathVision poses significantly higher difficulty for current VLMs, its average accuracy across models is around 30%, which suggests that models are often uncertain or guessing. In such low-performance regimes, prediction behaviors may become erratic or overly stochastic, reducing the reliability of entropy, correlation, and voting-based signals. As a result, the dependency measures may not reflect meaningful error structure, making MV behavior less predictable.

D.2 EMPIRICAL EVIDENCE TO SUPPORT ASSUMPTION

Fig. 8 shows the relationship between normalized entropy \tilde{H}_u and accuracy across multiple models on six benchmarks. We observe a strong inverse correlation between entropy and accuracy, consistent

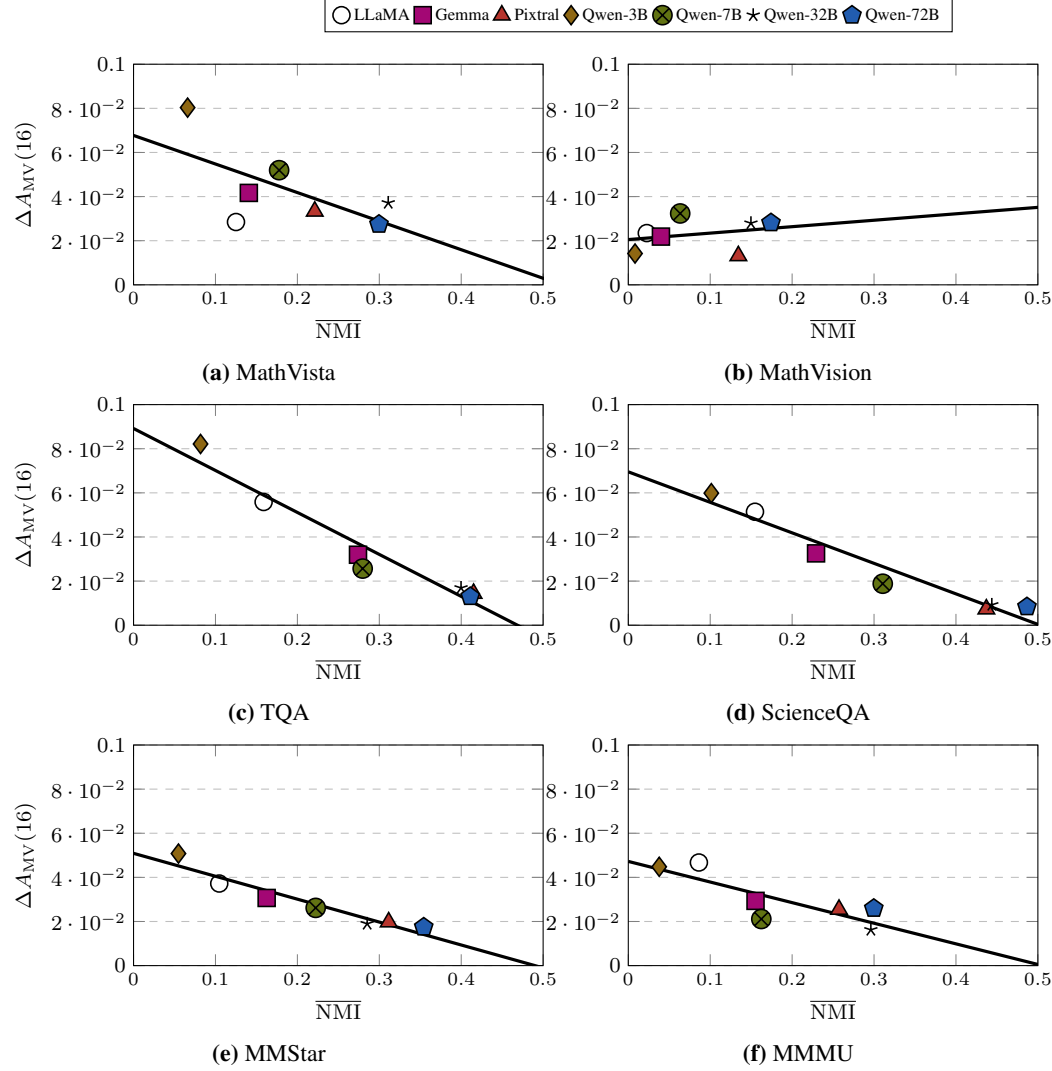


Figure 6: MV improvement $\Delta A_{MV}(16)$ plotted against average pairwise normalized mutual information (\overline{NMI}) for each model on each dataset. A negative trend suggests that higher prediction dependency reduces the benefit of majority voting.

with our Entropy-Accuracy Monotonicity assumption (Assumption 1). Higher-performing models generally exhibit lower entropy, indicating more confident and reliable predictions.

D.3 SUPERVISED ETTC

We provide additional details on the supervised variant of ETTC, which learns from a small set of labeled question–model pairs when low entropy is a *reliable* signal of correctness.

Problem setting. Given Q questions and M models, each model u produces a predictive distribution $p_{qu}(\cdot)$ over K options for question q , aggregated over $U=16$ stochastic decoding samples (see § 4). The goal is to learn a function that predicts whether a model’s low-entropy output is likely to be correct.

Feature construction. For each (q, u) pair, we compute two features:

$$\tilde{H}_{qu} := -\frac{1}{\log K} \sum_{k=1}^K p_{qu}(k) \log p_{qu}(k), \quad \text{RelEnt}_{qu} := \frac{\tilde{H}_{qu} - \min_v \tilde{H}_{qv}}{\max_v \tilde{H}_{qv} - \min_v \tilde{H}_{qv}}.$$

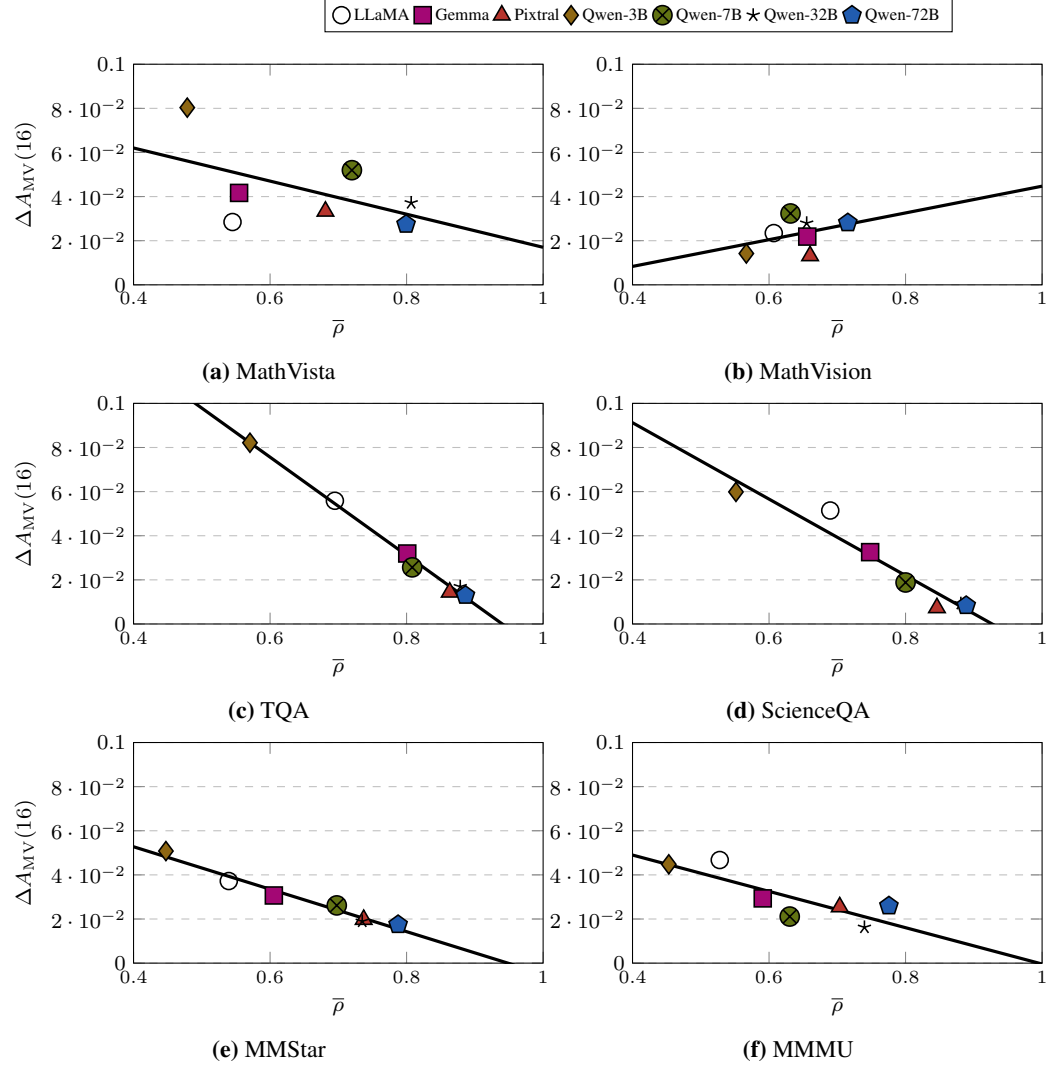


Figure 7: MV improvement $\Delta A_{\text{MV}}(16)$ versus average pairwise accuracy correlation $(\bar{\rho})$. Consistent with theory, stronger dependency (i.e., higher $\bar{\rho}$) corresponds to smaller gains from majority voting.

Here \tilde{H}_{qu} is the normalized entropy of model u , while RelEnt_{qu} contextualizes this entropy relative to other models for the same question. The final feature vector is $(\tilde{H}_{qu}, \text{RelEnt}_{qu}) \in \mathbb{R}^2$.

Labels and classifier. The binary label is

$$Z_{qu} := \mathbb{I}\{\hat{y}_{qu} = Y_q\},$$

where \hat{y}_{qu} is the top-1 prediction and Y_q is the ground truth. We train a logistic regression classifier to predict $\Pr(Z_{qu} = 1)$ from the entropy features.

Training protocol. To simulate low-resource conditions, we use two-fold cross-validation across questions: each dataset is split into halves, one for training and one for testing, with roles reversed in a second run. This prevents test leakage and mimics scenarios where only limited annotations are available.

Inference rule. At test time, for each (q, u) we compute the adjusted score

$$\text{Score}_{qu} := \tilde{H}_{qu} \cdot (1 - \hat{p}_{qu}),$$

where \hat{p}_{qu} is the predicted correctness probability from the classifier. We then select the model with the lowest score:

$$u_q^* := \arg \min_u \text{Score}_{qu}, \quad \hat{Y}_q := \hat{y}_{qu^*}.$$

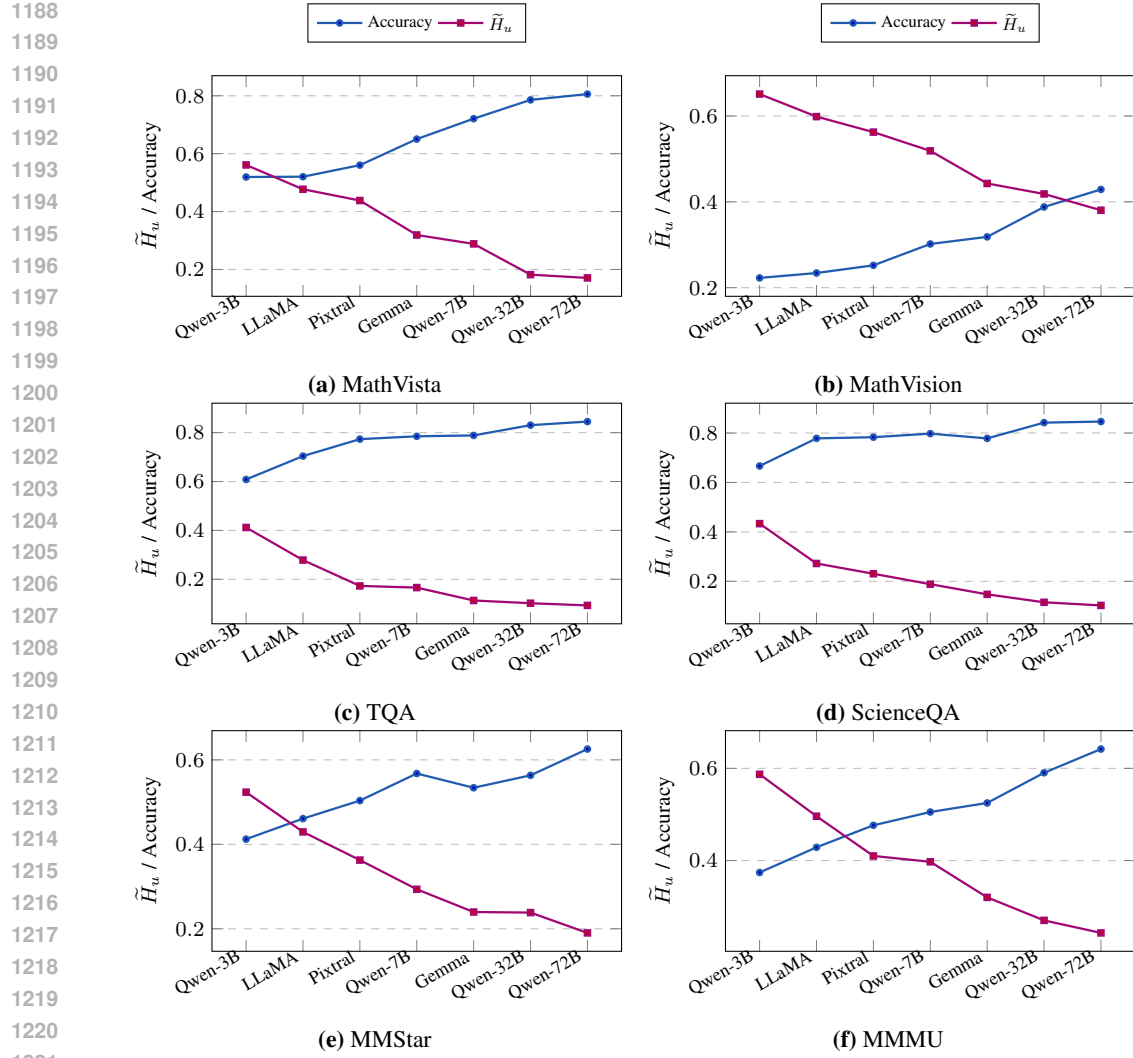


Figure 8: Correlation between normalized entropy \tilde{H}_u and accuracy across models on six benchmarks, supporting the Entropy–Accuracy Monotonicity assumption (Assumption 1).

This rule penalizes overconfident but unreliable predictions while rewarding trustworthy ones.

Table 7: Evaluation results across datasets for **Similar Size Models** and **Same Family Models**. Columns show the average single-model accuracy (Average), MV, (unsupervised) ETTC, and supervised variant of ETTC.

| Accuracy % | Similar Size Models | | | | Same Family Models | | | |
|----------------|---------------------|--------------|--------------|------------------------------|--------------------|--------------|--------------|------------------------------|
| | Avg. | MV | ETTC | Sup. ETTC $_{\Delta}$ | Avg. | MV | ETTC | Sup. ETTC $_{\Delta}$ |
| MathVista | 61.30 | 68.33 | 75.93 | 79.63 _{3.70↑} | 70.80 | 83.15 | 84.44 | 84.81 _{0.37↑} |
| MathVision | 27.66 | 32.05 | 35.57 | 36.62 _{1.05↑} | 33.53 | 41.32 | 44.84 | 46.34 _{1.50↑} |
| TQA | 76.28 | 83.65 | 83.90 | 84.14 _{0.24↑} | 76.73 | 84.90 | 86.70 | 86.70 _{0.00↑} |
| ScienceQA | 78.44 | 85.52 | 85.28 | 85.97 _{0.69↑} | 78.82 | 84.04 | 85.03 | 86.07 _{1.04↑} |
| MMStar | 51.65 | 59.27 | 60.07 | 60.67 _{0.60↑} | 54.22 | 61.00 | 63.73 | 65.07 _{1.34↑} |
| MMMU | 48.39 | 53.66 | 58.63 | 59.01 _{0.38↑} | 52.79 | 58.63 | 65.34 | 66.46 _{1.12↑} |
| Average | 57.29 | 63.75 | 66.56 | 67.67_{1.11↑} | 61.15 | 68.84 | 71.68 | 72.58_{0.90↑} |

1242 **Results.** As shown in Tab. 7, supervised ETTC outperforms both MV and unsupervised ETTC
1243 across datasets and ensemble settings. Gains are largest on ambiguous tasks (e.g., MathVision,
1244 MMStar, MMMU), where entropy alone is less reliable. Even with only two-fold cross-fitting and no
1245 extra supervision, the classifier learns to identify failure modes of entropy selection, making more
1246 robust choices and underlining the value of combining entropy with supervised error modeling.
1247

1248 LIMITATIONS

1250 Our study focuses on multiple-choice visual reasoning tasks and assumes access to model confidence
1251 scores via output distributions. The proposed methods, especially entropy-based selection, may not
1252 directly generalize to open-ended tasks or models lacking probabilistic outputs. Additionally, while
1253 our evaluation covers diverse datasets and model ensembles, the gains of supervised entropy-based
1254 TTC depend on the quality and availability of annotated examples, which may be costly to obtain in
1255 some domains. Lastly, our analysis assumes that entropy correlates with accuracy, which may not
1256 hold for all models or tasks.
1257

1258 LLM USAGE

1260 We used ChatGPT as general-purpose assistive tools during the preparation of this paper. Specifically,
1261 LLMs were employed for polishing grammar, improving clarity, formatting LaTeX, generating
1262 illustrative figures, and debugging minor code snippets. LLMs were not involved in research ideation,
1263 experimental design, or the development of theoretical results.
1264
1265
1266
1267
1268
1269
1270
1271
1272
1273
1274
1275
1276
1277
1278
1279
1280
1281
1282
1283
1284
1285
1286
1287
1288
1289
1290
1291
1292
1293
1294
1295